JOURNAL OF MATERIALS SCIENCE **40** (2005) 2951–2957

Synthesis and properties of β type $Bi(III)_{2-2x}Dy(II)_{2x}O_{3-x}\square_x$ solid solution

O. TURKOGLU
Department of Chemistry, Faculty of Arts and Sciences, Erciyes University, 38039 Kayseri-Turkey
E-mail: turkoglu@erciyes.edu.tr

M. ARI
Department of Physics, Faculty of Arts and Sciences, Erciyes University, 38039 Kayseri-Turkey

M. SOYLAK
Department of Chemistry, Faculty of Arts and Sciences, Erciyes University, 38039 Kayseri-Turkey

I. BELENLI
Department of Physics, Faculty of Arts and Sciences, Abant Izzet Baysal University, 14280 Bolu-Turkey

In the present work, tetragonal β type $Bi(III)_{2-2x}Dy(II)_{2x}O_{3-x}\square_x$ ($\square$: empty oxygen site) solid solutions have been synthesized in the ranges $0.06 \leq x \leq 0.08$ at 750°C and $0.05 \leq x \leq 0.09$ at 800°C by doping small amounts of Dy_2O_3 into monoclinic α-Bi_2O_3. X-ray powder diffraction (XRD) has been used for characterisation of the doped Dy_2O_3 powders as well as for calculation of the unit cell parameters. The polymorphic phase transitions, crystallographic properties, particle sizes, the scanning electron microscope (SEM) microprobe analysis and Dy_2O_3 content dependence of the lattice parameters of the observed β-phase has been reported. The obtained solid solutions had nonstoichiometric character and nonstoichiometry increases with the increasing amount of Dy_2O_3 addition. The experimental results suggested that oxygen vacancies are present in the crystal structure of Dy_2O_3 doped β type solid solutions.

1. Introduction

Bi_2O_3-based materials have been extensively investigated for a long time for applications in energy conversions, chemical processing, combustion controls, promoting heterogeneous catalytic reactions, solid oxide fuel cells [1–9]. Due to their oxygen ionic conductivity, they are used for producing oxygen sensors, oxygen pumps, oxygen-permeable membrane reactors and solid electrolytes of electrochemical cells. The operation of these devices with high efficiency requires a high temperature due to a utilisation of their high oxide-ion conductivity [1–3, 7–9]. Solid electrolytes such as polymorphs of Bi_2O_3 are essential components in the production of solid state electrochemical devices. They have also been used as the insulating coating materials for some superconductivity applications and production of Bi-based superconductors. In recent years, the development of new materials as alternatives to the traditional stabilized zirconias has taken place. These systems often show improved low-temperature conductivity compared to the stabilized zirconias [1–9].

Bi_2O_3 itself shows significant polymorphism, four polymorphs of bismuth trioxide have been reported in the literature, viz: α, δ, γ and β-phases [1, 2, 7, 9, 10]. The phase transition from the monoclinic α-phase, to the high temperature cubic (*fcc*) δ-phase, at approximately 730°C. The δ-phase is also stable up to its melting point of approximately 825°C. On cooling from the high temperature δ-Bi_2O_3 to room temperature, a large thermal hysteresis is observed, with the possible occurrence of two intermediate metastable phases, viz: the tetragonal β-phase or the cubic (*bcc*) γ-phase. The β-Bi_2O_3 occurs at approximately 650°C on cooling, while the γ-form is formed at approximately 640°C [8–10]. Usually these metastable phases transform to the α-phase below 500°C temperatures [8–10, 12]. On the other hand, the γ-Bi_2O_3 is also shown to persist to room temperature, when the cooling rate is kept very low [7–11]. The δ, β and γ-phases of bismuth oxide can be stabilized by addition of small amounts of other oxides such as ZrO_2, Y_2O_3, MoO_3, CoO, WO_3, SrO, CaO, La_2O_3, SeO_2, V_2O_5, Eu_2O_3, Gd_2O_3, Sm_2O_3 and Sb_2O_3 [1, 2, 7, 8, 10–21].

In this paper, we report on the effect of Dy_2O_3 doping in Bi_2O_3. After accomplishing the stability of Bi_2O_3 polymorphs by the solid state reactions, we have

determined lattice parameters at room temperature for each doping ratio. The solubility limits, colour changes, effects of heat treatment temperatures, and nonstociohometry of the obtained phases were investigated. Moreover, some crystallographic and microstructural properties of the obtained single β-phase samples were examined.

2. Experimental

The powder oxide mixtures of $(Bi_2O_3)_{1-x}(Dy_2O_3)_x$ system in the range $0.01 \leq x \leq 0.1$ have been prepared by mixing and homogenising the stoichiometric amounts of the monoclinic Bi_2O_3 (99.99% Merck) with Dy_2O_3 (99.99% Merck) in an agate mortar. These powder mixtures were firstly heated at 650°C for 48 h. The pre-annealed powders were ground and then annealed each from 50°C up to 800°C for 48 h with several intermediate grindings. After these heat treatments oxide powders were heat treated further at 825°C (around melting point of bismuth trioxide) for 24 h. All these heat treatments were performed as loose powders, in alumina crucibles, in air and without any compaction. At the end of each heat treatment procedure, annealed powders were slowly cooled in the furnace by switching it off (uncontrolled). Each of these prepared powder samples were heat treated separately at 825°C in a vertical tube furnace in air, and quenched by suddenly dropping the sample into ice-water mixture which was prepared from double distillate water. Quenching experiments were performed to observe high temperature phase transitions in the synthesized samples with Dy_2O_3 to Bi_2O_3 addition ratio. The colour changes of the obtained single-phases were determined carefully depending on the Dy_2O_3 additions, and heat treatment temperatures (on the disk shape samples, diameter 10 mm, thickness 0.4 mm, in a stainless holder $\sim$1000 kgf cm^{-2}).

The X-ray powder diffraction (XRD) data of the samples were recorded on a computer-interfaced Bruker AXS D8 advanced diffractometer operating in a Bragg-Brentano geometry (CuK_α radiation, graphite monochromator, 40 kV and 40 mA) over a $10^\circ \leq 2\,\theta \leq 90^\circ$ angular range. The divergence and receiving slits of 1 and 0.1 mm, respectively, were located on the diffractometer. Diffraction patterns were scanned by 0.002° (2θ) steps and diffracted beams were counted with a NaI(Tl) scintillation detector. Measured XRD patterns were readily compared with the reference data [22].

Microprobe analysis of formed tetragonal type samples were carried out by LEO 440 scanning electron microscope (SEM). Microprobe analysis data were taken from flat surface of the pressed samples. At least five different analysis were made from different regions of each sample at high magnification and mean values from these measurements were used for calculations. Particle sizes of the obtained β type samples at various heat treatment temperatures were determined using XRD data and the Scherrer and Warren equations [24]:

$$S = 0.9\lambda/(B\cos\theta_B)$$

where λ is the wavelength of the X-ray source, S is the grain size of the crystallite, θ_B is the Bragg angle of the considered XRD peaks, and B represents the fwhm line broadening obtained as follows:

$$B^2 = B_m^2 - B_s^2$$

where B_m^2 is the fwhm line broadening of the material and B_s^2 represents the fwhm line broadening of the internal standard (α-Al_2O_3). In this study, the values of crystallite sizes obtained from the (201), (002), (220) and (222) planes which have the strongest diffraction peak intensities by using Bruker AXS D8 TOPAS 2 software [24].

3. Results and discussion

The observed single-phases and heterogeneous solid mixtures in the $(Bi_2O_3)_{1-x}(Dy_2O_3)_x$ system, depending on the reaction temperature, are given in Table I. The XRD patterns completed on the samples after firing at 700°C showed that a range of mixture of α and β-phases. The dominant single-phase regions have synthesized the tetragonal β-Bi_2O_3 type crystal structure. 750°C was the minimum temperature at which the β-phase was obtained from furnace cooled specimens in the range of $0.06 \leq x \leq 0.08$ and at 800°C, x was between 0.05 and 0.09 additions of Dy_2O_3. In these doping ranges, all of the observed XRD pattern peaks were indexed in the tetragonal type unit cell. The XRD patterns of 7 mol% Dy_2O_3 addition (after firing at 750 and 800°C for 48 h) are given in Fig. 1. The XRD patterns of the other single β-phase samples were quite similar to the patterns of the single phase sample given in this figure. The XRD measurements revealed that doping with more than 8 or 9 mol% Dy_2O_3 and less than 5 or 6 mol% Dy_2O_3, depending on the heat treatment temperature, had produced the heterogeneous mixture

TABLE I The observed phases in the system of $(Bi_2O_3)_{1-x}(Dy_2O_3)_x$; x being $0.01 \leq x \leq 0.1$

	Mol% Dy_2O_3 addition									
Temperature (°C)	1	2	3	4	5	6	7	8	9	10
700	$\alpha+\beta$	$\alpha+\beta$	$\alpha+\beta$	$\alpha+\beta$	$\alpha+\beta$	$\alpha+\beta$	$\alpha+\beta$	$\alpha+\beta$	$\alpha+\beta$	$\alpha+\beta$
750	$\alpha+\beta$	$\alpha+\beta$	$\alpha+\beta$	$\alpha+\beta$	$\alpha+\beta$	β	β	β	$\alpha+\beta$	$\alpha+\beta$
800	$\alpha+\beta$	$\alpha+\beta$	$\alpha+\beta$	$\alpha+\beta$	β	β	β	β	β	$\alpha+\beta$
825	$\alpha+\gamma$	$\alpha+\gamma$	γ	γ	$\gamma+\beta$	$\gamma+\beta$	$\gamma+\beta$	$\gamma+\beta$	$\gamma+\beta$	$\gamma+\beta$
825 wq[a]	$\alpha+\beta$	$\alpha+\beta$	$\alpha+\beta$	$\alpha+\beta$	$\alpha+\beta$	$\alpha+\delta$	$\alpha+\delta$	$\alpha+\delta$	δ	δ

[a]Water quench.

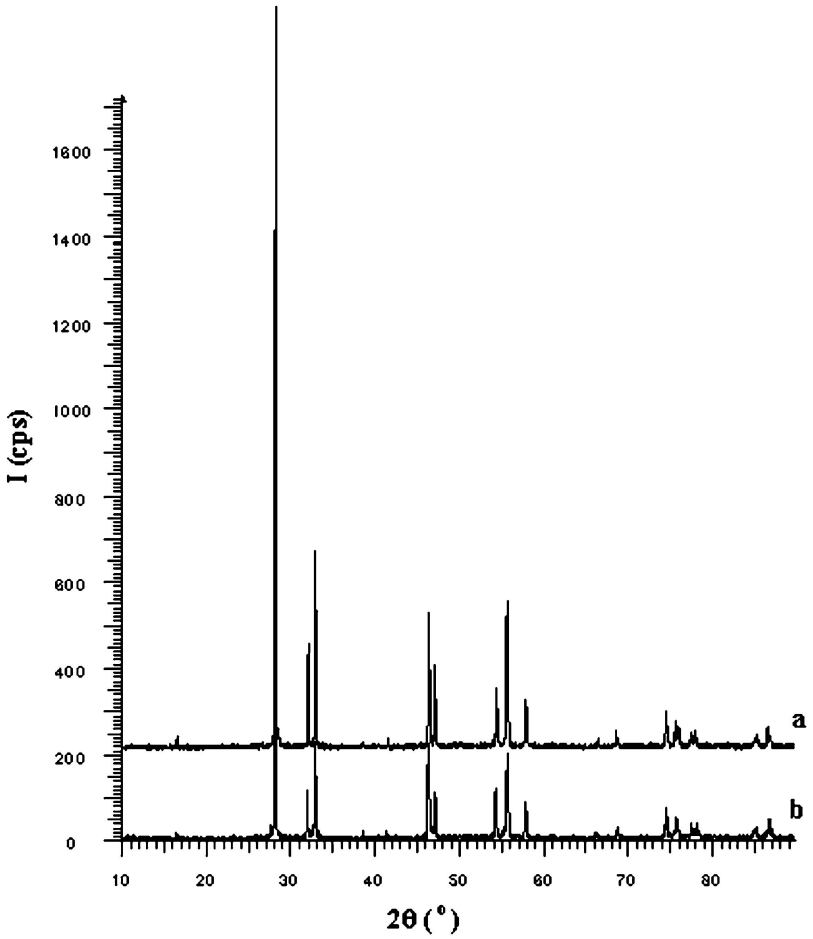

Figure 1 XRD patterns of β-Bi_2O_3 doped with 7 mol% Dy_2O_3: (a) after heating at 800°C, (b) after heating at 750°C.

of α and β forms. XRD patterns of some of the multiphase samples are given in Fig. 2 and assignments of individual peaks to α, β, γ or δ- phases were indicated on the patterns.

The unit cell parameters (a and c) of the β-phase increasing slightly with increasing Dy_2O_3 content (Fig. 3) in good agreement with effective ionic radii considerations. The reported ionic radii (6-coordinated) are 0.102 nm for Bi^{3+}, 0.121 nm for Dy^{2+} and 0.105 nm for Dy^{3+}, based on 0.140 nm for the O^{2-} ion [23]. When the Dy^{2+} ions replace the Bi^{3+}cations, the lattice parameters expand (Bi^{3+} ion has smaller ionic radii than Dy^{2+}) and these enlargements are consistent with our observations on the lattice parameters changes. It was also observed that the lattice parameters of the same composition differ for various heat treatment temperatures, being slightly larger for 800°C, compared to for 750°C. The solid solutions of Bi_2O_3 and Dy_2O_3 were obtained as single β-phase in the range of 6–8 mole % Dy_2O_3 addition, when the oxide mixtures are heat treated at 750°C. The solubility range widens when the heat treatment temperature is increased to 800°C, being 5–9 mol%. In Fig. 3, it is also suggested that the solubility limits of Dy_2O_3 in the β-Bi_2O_3 phase are around 9 mol% at 800°C and 8 mol% at 750°C. This experimental observation is explained with insufficient solid state reaction at 750°C, rather than solubility limitation. This is conclusive with larger unit cell parameters at higher annealing temperatures for the same compositions as out lined above.

On the other hand, the formation of the tetragonal type $(Bi_2O_3)_{1-x}(Dy_2O_3)_x$ solid solution was a very slow process requiring a long heat treatment. It was concluded from this fact that the diffusion rate for the dysprosium ions into bismuth trioxide was quite low. Through this slow diffusion mechanism, the Dy cations substitute the Bi ions in the crystal structure. Although the valence number of the Dy cation is 3+ in Dy_2O_3, those incorporated in the Dy ions would probably be reduced to bivalent in that obtained from the tetragonal type solution. When the charge balance is considered, as the addition of Dy_2O_3 increases, the O^{2-} ions should spontaneously be oxidized to O_2 molecules. Then, some oxygen ion vacancies should occur in the O^{2-} sublattices of the tetragonal $(Bi_2O_3)_{1-x}(Dy_2O_3)_x$ solution. As a result, the obtained solid solution acquires nonstoichiometric character. The nonstoichiometry for formed samples in this study can be regarded as an oxygen vacancy type as seen in the other studies [2, 7–10, 15–19, 25–28]. Therefore, the composition of the β-type solid solution can be expressed as

$$Bi(III)_{2-2x}Dy(II)_{2x}O_{3-x}\square_x$$

where □ denotes the vacancy of oxygen ion. x values are in $0.06 \leq x \leq 0.08$ range for heat treatment at 750°C and they are in the range of $0.05 \leq x \leq 0.09$ for heat treatment at 800°C.

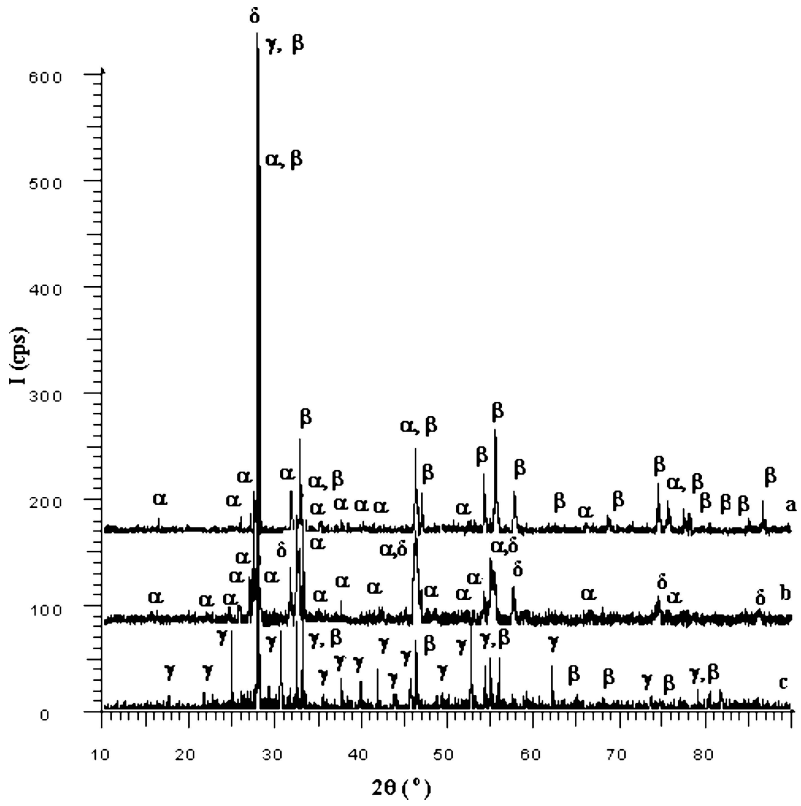

Figure 2 XRD patterns of some of the multiphase samples. (a) 4 mol% Dy_2O_3 addition (after heating at 750°C), (b) 7 mol% Dy_2O_3 addition (after quenching at 825°C), (c) 5 mol% Dy_2O_3 addition (after heating at 825°C).

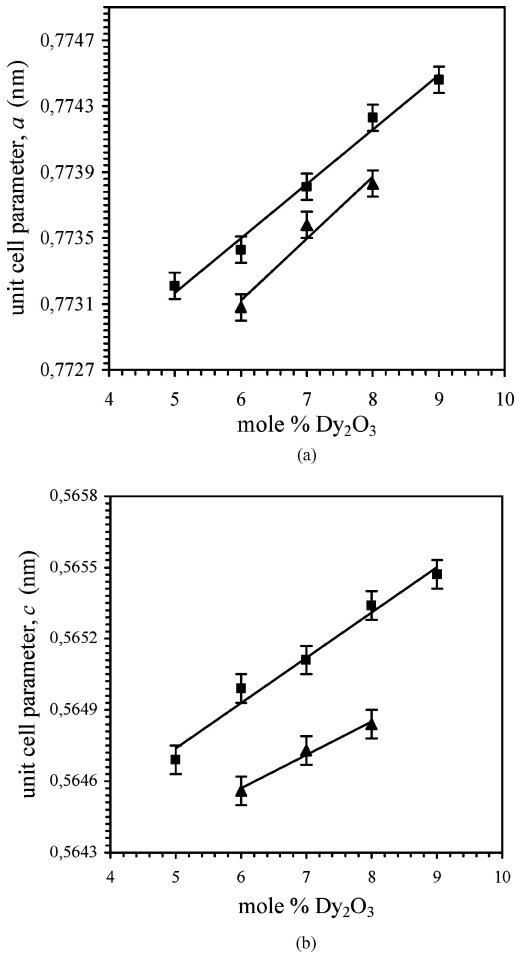

Figure 3 The relationship between the amount of Dy_2O_3 doping, and the lattice parameter of β type solid solution; (a) Unit cell parameter a, (b) Unit cell parameter c (■ : after heating at 800°C, ▲ : after heating 750°C).

The calculated weight ratio values of elements, obtained using the approximations outlined above, are given in Table II. The values of wt% Bi and wt% Dy were calculated according to nonstoichiometric theoretic formula [15, 16]. The weight ratio values measured by using SEM microprobe analysis are also given in Table II. These measured values are in good agreement with the calculated ones. The cation concentrations are higher than the expected stoichiometric values, indicating the oxygen vacancies in this phase were considered to distribute randomly. Although, this is not a solid proof for the oxygen deficiency, it nevertheless is in agreement with the cited literature [7, 10, 15, 16, 25, 26]. This oxygen deficiency can lead to variations in the electrical conductivity properties of these doped samples [1, 2, 11–13].

The observed colour of the β-phase samples had a systematic change depending on the amount of Dy_2O_3 addition. The colours of the sintered specimens were observed only light yellow colour for the multiphase ($\alpha + \beta$) samples. On the other hand, as β type solid solution is formed with increasing addition ratio, the colour of the disks changed to red brown which is a darker colour. The colour varying phenomenon may be considered to be related to the degree of nonstoichiometry. Also, the observed color change may be attributed to a charge transfer between the oxide ions and vacancies. The existence of O^{2-} vacancies in the crystal structure can also contribute to the colour; because vacancy points maybe occupied by electrons through a light absorption mechanism.

The results of the grain size calculations from XRD data are shown in Table III. There is a general tendency that grain size becomes smaller with increasing addition

TABLE II The microprobe analysis for the tetragonal (β) type solution of $(Bi_2O_3)_{1-x}(Dy_2O_3)_x$ system

	After heating at 750°C		After heating at 800°C		Calculated	
x (Dy_2O_3) (mol%)	wt% Bi	wt% Dy	wt% Bi	wt% Dy	wt% Bi	wt%Dy
0.05	(−)[a]		86.34 ± 0.21	3.48 ± 0.10	86.23	3.53
0.06	86.12 ± 0.22	3.94 ± 0.19	85.49 ± 0.23	4.30 ± 0.14	85.52	4.25
0.07	84.42 ± 0.19	4.73 ± 0.27	84.91 ± 0.26	4.91 ± 0.11	84.81	4.96
0.08	85.27 ± 0.31	5.79 ± 0.23	84.14 ± 0.27	5.57 ± 0.13	84.10	5.69
0.09	(−)[a]		83.53 ± 0.29	6.37 ± 0.11	83.39	6.41

[a]Single β phase could not be observed.

TABLE III Effect of doping ratio of Dy_2O_3 on grain size for the planes (nm)

	After heating at 750°C				After heating at 800°C			
x (Dy_2O_3) (mol%)	(201)	(002)	(220)	(222)	(201)	(002)	(220)	(222)
0.05		(−)[a]			125.3	144.8	97.2	114.8
0.06	139.8	155.9	94.5	111.9	117.1	136.6	88.8	98.3
0.07	126.4	122.5	89.6	101.1	109.4	114.7	71.3	79.7
0.08	104.2	112.9	69.7	91.7	107.4	102.1	60.1	62.2
0.09		(−)[a]			95.6	88.3	57.4	52.9

[a]Single β phase could not be observed.

ratio. The sharpest and symmetrical peaks were used for calculations and the (201) plane has the highest intensity. We have also observed that grain sizes of the samples annealed at 800°C are slightly smaller than the samples annealed at 750°C.

Previously reported studies of Bi_2O_3 polymorphs show that the unit cell parameters of the nonstoichiometric phase β-$Bi_2O_{2.5}$ are $a = 0.750$ nm and $c = 0.563$ nm in the space group $P42_{1c}$ [2]. The locations of the bismuth ions in the crystal structures of the stoichiometric and nonstoichiometric bismuth three oxides are almost identical while locations of the oxygen ions exhibit differences. For stoichiometric compounds of this type, all particular cationic and anionic sites in the tetragonal crystal system are fully occupied. The nonstoichiometric β-phase has the oxygen ion vacancies in the crystal structure [10, 25, 26]. The calculated lattice parameter values of the observed β-type solid solutions (see Fig. 3) are in agreement with the unit cell parameters of the β-$Bi_2O_{2.5}$ phase [26], indicating oxygen nonstoichiometry in the synthesized tetragonal solid solutions. The higher doping rates introduce more defects into the structures, hence tetragonality is enhanced.

Another polymorph γ-phase was prepared from the samples of 3 and 4 mol% Dy_2O_3 additions by heating at 825°C (around melting point) then furnace cooled (slow cooling) samples. Measured XRD patterns of 4 mol% Dy_2O_3 sample was given in Fig. 4. The XRD pattern peaks of these samples were indexed in the body centred cubic crystal symmetry. This phase could not be obtained with lower and higher Dy_2O_3 concentrations, and the other heat treatments. The colours of produced samples were orange yellow. The observed colour change may be attributed to a charge transfer between the oxide ions and vacant orbital of Dy^{2+} cations. Indeed, most of the metal oxides with high oxidation numbers are coloured and these colours also stem from the charge transfer mechanism. In other words, the oxygen lattice points of the Dy_2O_3 doped γ-phase are not completely occupied with oxygen ions. It was considered that the changing of the colour occurs depending on the nonstoichiometry in the crystal structures of γ-Bi_2O_3 type solid solution. As a result of these, oxygen vacancies are partly responsible for nonstoichiometry in our bulk samples. Some of measured XRD patterns of $\alpha + \gamma$ and $\gamma + \beta$ multi-phases samples are also shown in Fig. 4. The lattice parameters, a, of the *bcc* materials were found $a = 1.02149$ nm and $a = 1.02063$ nm for $x = 0.03$ and $x = 0.04$ additions of Dy_2O_3, respectively. According to our literatures surveys [7, 12, 25, 26], the pure γ-Bi_2O_3 contains $Bi_{26}O_{39}$ in the cell with lattice parameters in the range of 1.010–1.027 nm. γ-Bi_2O_3 has the largest unit cell parameter of the series of the reported Sillenite group compounds [7, 12, 25, 26]. Other investigators [7, 10, 12, 25, 26], suggest that the γ-Bi_2O_3 phase is also reported to be isomorphous with several other metal oxides giving the general formula $Bi_{24}M_2O_{39}$. The M cations are tetrahedrally coordinated and occupy the body centred sites and cube corners linked by hepta coordinated bismuth atoms. The Bi_2O_3 host lattice forms a cage type structure that can accommodate small metal ions in a tetrahedral coordination of oxygen atoms. For nonstoichiometric compounds, metal ions are not quadrivalent so that the structure should contain fractionally occupied sites. In other words, γ-Bi_2O_3 has some oxygen ion vacancies in structure that is described as the distorted defect crystal structure. On the other hand, crystal lattice has the perfect structure where the M cation is tetravalent giving the general formula $Bi_{24}M_2O_{40}$ in the unit cell. Thus, for stoichiometric compounds of γ-form, all of the lattice points of the crystal structure are fully occupied by cations and anions.

The δ-phase was prepared from the samples of 9–10 mol% Dy_2O_3 addition by melting at 830°C then fast

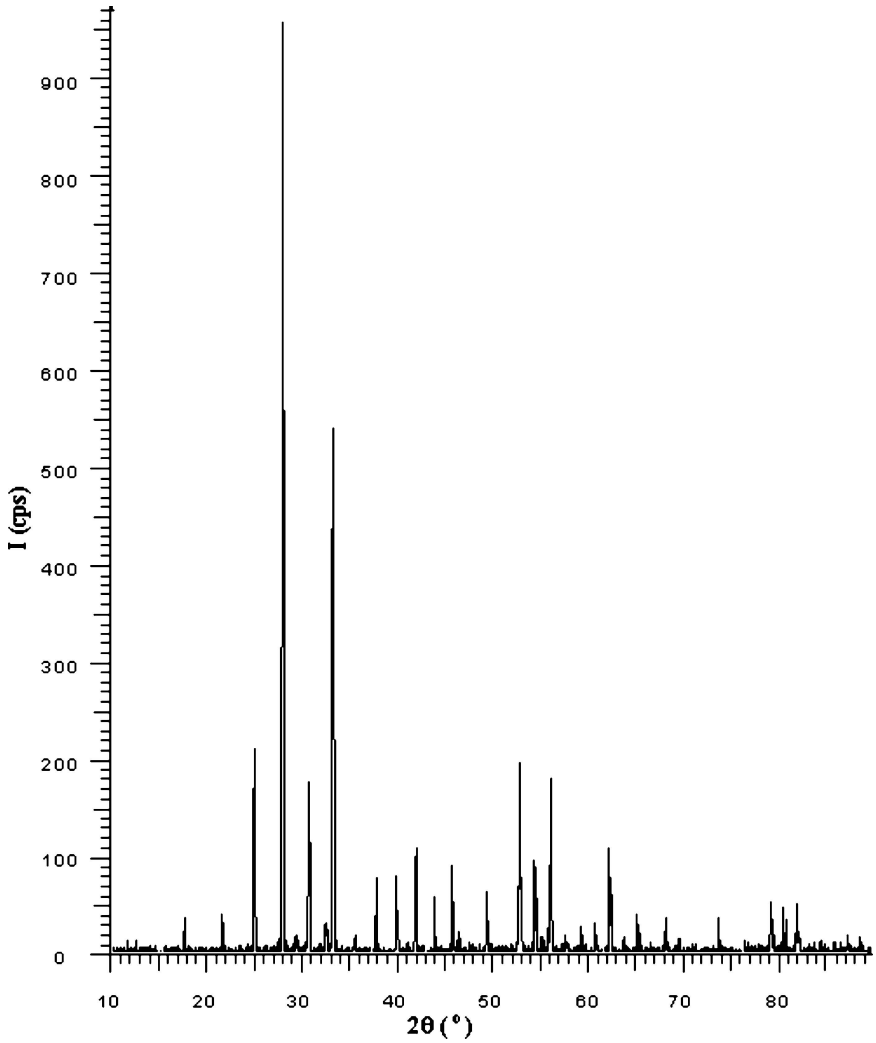

Figure 4 XRD pattern of γ-Bi_2O_3 doped with 4 mol% Dy_2O_3 after heating 830°C.

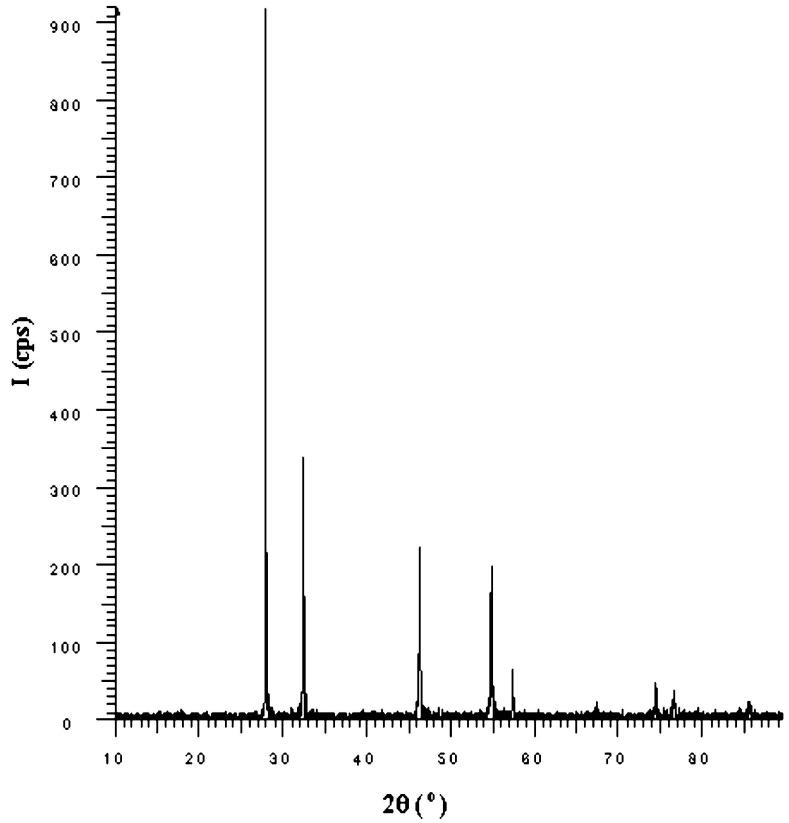

Figure 5 XRD pattern of δ-Bi_2O_3 doped with 9 mol% Dy_2O_3 after heating 830°C.

quenching to 0°C in the water-ice system. Below the 9 mol% doping level, led to coexistence a solid mixture of δ and γ-phases. The XRD peaks of the 9–10 mol% samples were indexed in the face centred cubic crystal system. XRD pattern of 9 mol% Dy_2O_3 material is seen in Fig. 5. The unit cell constants were calculated $a = 0.55321$ nm, and $a = 0.55358$ nm for 9 and 10 mole percentage additions of Dy_2O_3 respectively. This was an indication that Dy_2O_3 dissolves in δ type Bi_2O_3 matrix. In the references [15, 17], the *fcc* form has an oxygen deficient fluorite structure with two formula units, and two oxygen ion vacant sites per unit cell. The unit cell parameter is $a = 0.566$ nm, with a *Pn*3*m* space group and bismuth ions in the structure are located on *fcc* sites, and differ only in the location of the oxygen ions [15, 17].

4. Conclusions

Metastable β, γ, and δ-phases of Bi_2O_3 polymorphs and related solid solutions have been obtained as room temperature stable phases by doping pure monoclinic α-Bi_2O_3 material with Dy_2O_3, and employing solid state reaction techniques. Heat treatment temperature, heating time, cooling rates, and amount of Dy_2O_3 are effective factors in the synthesis of these polymorphs. On the other hand, formation of β, γ, and δ-phases were very slow requiring high temperatures, and long time heat treatments. Diffusion rate for dysprosium ions into bismuth trioxide was quite low. Through this slow diffusion mechanism, Dy^{3+} cations are reduced to Dy^{2+} ions which are substituted bismuth cations in the tetragonal crystal structure. During this reduction mechanism, the O^{2-} ions in the crystal lattice have been oxidized to oxygen molecules. Those reduction and oxidation reactions have been caused O^{2-} vacancies in the tetragonal unit cell and nonstoichiometry. The synthesized β-phase has distorted defect crystal structures and some of the oxygen ions move to vacancies. Higher doping rates introduce more defects into the structures, and the most predominant defects are oxygen vacancies, which increase with increasing the amount of Dy_2O_3. Therefore, β-phase shows a relatively high oxygen ionic electrical conduction which is required for the solid electrochemical cell device performance. For that reasons, the synthesized phases, especially β-phase, can be used in some solid electrolytic industrial applications, for example, to fabricate oxygen detectors.

Acknowledgement

The authors would like to thank the Scientific and Technical Research Council of Turkey (TUBITAK) for financial helps (Project No: TBAG-2443 (104T052)).

References

1. T. TAKAHASHI, T. ESAKA and H. IWAHARA, *J. App. Electrochem.* **7** (1977) 31.
2. M. MIYAYAMA, S. KATSUTA, Y. SUENAGA and H. YANAGIDA, *J. Am. Ceram. Soc.* **66** (1982) 585.
3. G. CHIODELLI, A. MAGISTRIS, G. SPINOLO, C. TOMASI, V. ANTONUCCI and N. GIORDANO, *Solid State Ionics* **74** (1994) 37.
4. N. ARORA, G. DEO, I. E. WACHS and A. M. HIRT, *J. Catal.* **159** (1996) 1.
5. D. SREENNIVASU and V. CHANDRAMOULI, *Bull. Mater. Sci.* **23** (2000) 509.
6. I. BELENLI and O. TURKOGLU, *Supercond. Sci. Technol.* **16** (2003) 39.
7. O. TURKOGLU and I. BELENLI, *J. Therm. Anal. Calorim.* **73** 1001 (2003) 1001.
8. N. JIANG, E. D. WACHSMAN and S. JUNG, *Solid State Ionics.* **150** (2002) 347.
9. T. SHIDO, G. OKITA, K. ASAKURA and Y. IWASAWA, *J. Phys. Chem. B* **104** (2000) 12263.
10. H. A. HARWIG and A. G. GERARDS, *J. Solid State Chem.* **26** (1978) 265.
11. S. BOYAPATI, E. D. WACHSMAN and B. C. CHAKOUMAKOS, *Solid State Ionics*. **138** (2001) 293.
12. M. MIYAYAMA and H. YANAGIDA, *J. Mater. Sci.* **21** (1986) 1233.
13. E. ONIYAMA and P. G. WAHLBECK, *J. Phys. Chem. B.* **102** (1998) 4418.
14. M. R. FRANCE, J. W. BUCHANAN, J. C. RONINSON, S. H. PULLINS, J. L. TUCKER, R. B. KING and M. A. DUNCAN, *ibid. A* **101** (1997) 6214.
15. O. TURKOGLU, F. ALTIPARMAK and I. BELENLI, *Chem. Pap.* **57** (2003) 304.
16. O. TURKOGLU, M. SOYLAK and I. BELENLI, *Bull. Mater. Sci.* **25** (2002) 583.
17. O. TURKOGLU and M. SOYLAK, *Asian. J. Chem.* **14** (2002) 1698.
18. O. TURKOGLU, "The Investigation of the Phase Diagram of the Binary System of Bi_2O_3-Sb_2O_3", Ph.D. Thesis, Erciyes University, Kayseri-Turkey, 1995.
19. K. R. KENDALL, C. NAVAS, J. K. THOMAS and H.-C. LOYE, *Chem. Mater.* **8** (1996) 642.
20. ST. YORDANOV, Y. DIMITRIEV, Y. IVANOVA and L. LAKOV, *J. Therm. Anal. Calorim.* **65** (2001) 971.
21. S. EKHELIKAR and G. K. BICHILE, *Bull. Mater. Sci.* **27** (2004) 19.
22. Bruker AXS GmbH, Diffracplus PDF Maint Powder Diffraction Database Manager Software (2001).
23. A. R. WEST, "Basic Solid State Chemistry" (Wiley, New York, 1988).
24. Bruker AXS GmbH, Bruker AXS D8 TOPAS 2 Software (2001).
25. H. A. HARWIG, *Z. Anorg. Allg. Chem.* **444** (1978) 151.
26. J. W. MEDERNACH and R. L. SNYDER, *J. Am. Ceram. Soc.* **61** (1978) 494.
27. N. I. MEDVEDA, V. P. ZHUKOV and V. A. GUBANOV, *Sov. Phys. Solid State* **32** (1990) 1087.
28. G. GATTOW and D. SCHUTZE, *Z. Anorg. Allg. Chem.* **328** (1964) 44.

Received 20 August 2004
and accepted 6 January 2005